Behavioral/Cognitive

α Power Modulation and Event-Related Slow Wave Provide Dissociable Correlates of Visual Working Memory

Keisuke Fukuda,[1] Irida Mance,[2] and Edward K. Vogel[3]

[1]Department of Psychological Sciences, Vanderbilt Vision Research Center, Center for Integrative and Cognitive Neuroscience, Vanderbilt University, Nashville, Tennessee 37240, [2]Department of Psychology, University of Oregon, Eugene, Oregon 97403, and [3]Department of Psychology, University of Chicago, Chicago, Illinois 60637

Traditionally, electrophysiological correlates of visual working memory (VWM) capacity have been characterized using a lateralized VWM task in which participants had to remember items presented on the cued hemifield while ignoring the distractors presented on the other hemifield. Though this approach revealed a lateralized parieto-occipital negative slow wave (i.e., the contralateral delay activity) and lateralized α power modulation as neural correlates of VWM capacity that may be mechanistically related, recent evidence suggested that these measures might be reflecting individuals' ability to ignore distractors rather than their ability to maintain VWM representations. To better characterize the neural correlates of VWM capacity, we had human participants perform a whole-field VWM task in which they remembered all the items on the display. Here, we found that both the parieto-occipital negative slow wave and the α power suppression showed the characteristics of VWM capacity in the absence of distractors, suggesting that they reflect the maintenance of VWM representations rather than filtering of distractors. Furthermore, the two signals explained unique portions of variance in individual differences of VWM capacity and showed differential temporal characteristics. This pattern of results clearly suggests that individual differences in VWM capacity are determined by dissociable neural mechanisms reflected in the ERP and the oscillatory measures of VWM capacity.

Key words: **α oscillations; event-related potentials; human electrophysiology; individual differences; visual working memory**

Significance Statement

Our work demonstrates that there exist event-related potential and oscillatory correlates of visual working memory (VWM) capacity even in the absence of task-irrelevant distractors. This clearly shows that the two neural correlates are directly linked to maintenance of task-relevant information rather than filtering of task-irrelevant information. Furthermore, we found that these two correlates show differential temporal characteristics. These results are inconsistent with proposals that the two neural correlates are byproducts of asymmetric α power suppression and indicate that they reflect dissociable neural mechanisms subserving VWM.

Introduction

Visual working memory (VWM) enables us to maintain a limited amount of visual information in an active state (Luck and Vogel, 1997; Rouder et al., 2008; Zhang and Luck, 2008). Recently, many human electroencephalogram (EEG) studies of VWM have used lateralized displays and examined the neural activity in the hemisphere that is contralateral to the position of the remembered items. For example, Vogel and Machizawa (2004) had participants remember multiple objects presented on a cued visual field, while ignoring the distractors in the opposite visual field. Using the event-related potential (ERP) technique, they observed a sustained negative wave over the posterior electrode sites in the contralateral hemisphere, referred to as the contralateral delay activity (CDA). CDA amplitude showed a capacity-limited bilinear function that increased with set size up to each individual's capacity limit with no further increase for larger set sizes (Vogel and Machizawa, 2004). Similarly, recent studies examining oscillatory correlates of VWM capacity revealed that parieto-occipital α power was lower on the contralateral hemisphere than the ipsilateral hemisphere and that the magnitude of this power reduction showed a capacity-limited bilinear function with set size (Sauseng et al., 2009).

Received Dec. 8, 2014; revised Aug. 28, 2015; accepted Sept. 1, 2015.

Author contributions: K.F., I.M., and E.K.V. designed research; K.F. and I.M. performed research; K.F. and I.M. analyzed data; K.F., I.M., and E.K.V. wrote the paper.

This work was supported by NIH Grant R01-MH087214 and Office of Naval Research Grant N00014-12-1-0972 to E.K.V. We also thank Ali Mazaheri and an anonymous reviewer for providing helpful comments to improve this manuscript.

The authors declare no competing financial interests.

Correspondence should be addressed to Keisuke Fukuda, Department of Psychology, Vanderbilt University, PMB 407817, 2301 Vanderbilt Place, Nashville, TN 37240-7817. E-mail: keisuke.fukuda@vanderbilt.edu.

DOI:10.1523/JNEUROSCI.5003-14.2015

Copyright © 2015 the authors 0270-6474/15/3514009-08$15.00/0

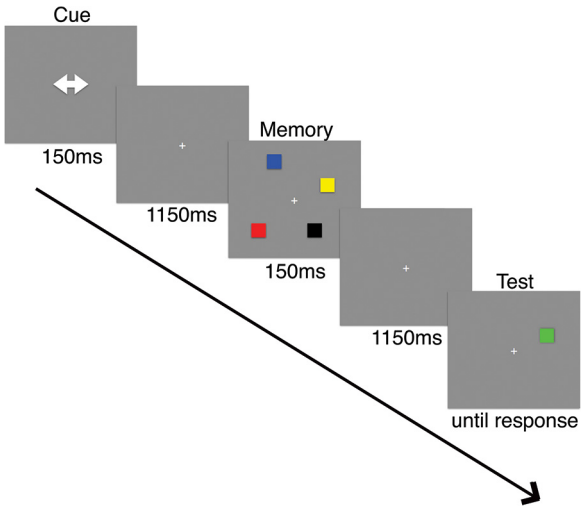

Figure 1. Whole-field change detection task.

Moreover, Jensen and colleagues (Mazaheri and Jensen, 2008; van Dijk et al., 2010) proposed that lateralized negative slow waves, such as the CDA, could be produced by an asymmetric modulation of lateralized α activity. Together, these results suggest that the capacity-defined modulation of the CDA and the lateralized α effect might reflect the same neural mechanism of VWM capacity.

The traditional approach using the lateralized VWM task has one primary disadvantage. In this paradigm, as the number of to-be-remembered items increases, there is a concurrent increase in the number of to-be-ignored items on the unattended side. Individuals with low VWM capacity are less efficient at ignoring distractors than high-capacity individuals (Vogel et al., 2005; McNab and Klingberg, 2008; Fukuda and Vogel, 2009, 2011). Thus, lateralized neural correlates of VWM capacity may in part reflect individuals' ability to ignore the distractors presented on the uncued side rather than solely their ability to maintain targets in VWM (Sauseng et al., 2009; Fukuda et al., 2015). Here, we used a task in which subjects must remember the items across both visual fields with no accompanying distractors and examined two primary questions regarding the neural correlates of VWM capacity. First, do the parieto-occipital negative slow wave and the α power show the capacity-defined set-size function in the absence of task-irrelevant distractors? If these signals truly reflect the capacity of VWM maintenance, they should still show the capacity-defined set-size functions. Second, is the α power modulation directly involved in generation of the negative slow wave of the ERP? If so, we should expect a significant correlation between the two measures.

Materials and Methods

Overview

Across two experiments, we used a standard change detection task in which participants remembered all the items presented across the entire visual field.

Participants

After obtaining informed consent following procedures approved by the University of Oregon, 33 (19 males) and 19 (11 males) university students with normal or corrected-to-normal vision participated in the study in return for $10 per hour for Experiments 1 and 2, respectively. Five subjects were removed from Experiment 1 because of too many rejected trials attributable to ocular artifacts (>40% of trials).

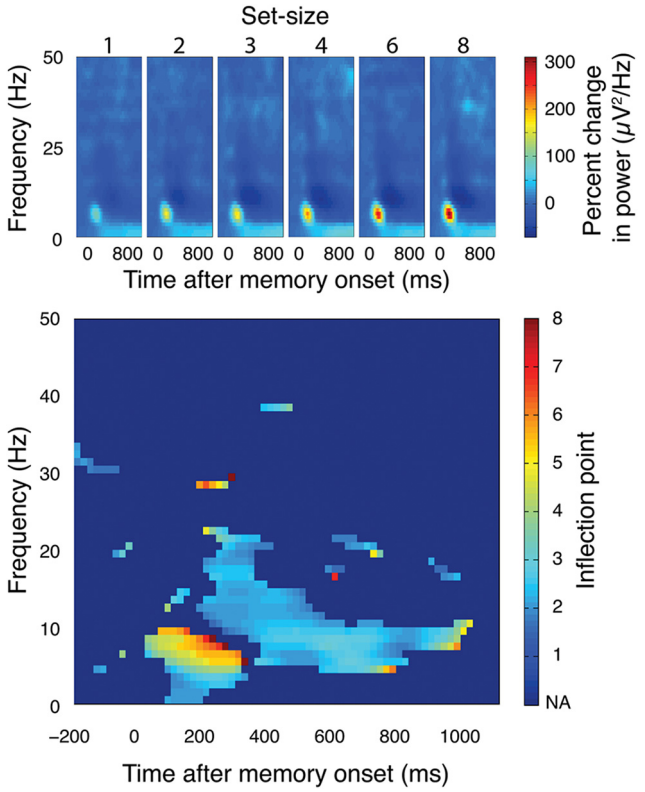

Figure 2. Time-frequency analyses in Experiment 1. Top, Event-related percent change in power in the frequency range of 0–50 Hz for each set size observed at a parieto-occipital channel (PO4). Bottom, Inflection point of the best-fitting bilinear function ($r > 0.9$) for a parieto-occipital channel (PO4).

Experiment 1

Behavioral procedure. Participants performed a whole-field change detection task (Fig. 1). Participants initiated each trial using a button press; at 1300 ms after the button press, a bidirectional arrow was presented at the center of the screen for 150 ms as a warning cue for onset of the upcoming memory array. At 1300 ms after the onset of the cue, a memory array that consisted of one, two, three, four, six, or eight colored squares was presented for 150 ms. The memory array was created from nine highly discriminable colors (red, green, blue, yellow, magenta, cyan, orange, black, and white) that were randomly chosen without replacement. Participants were asked to remember as many colored squares as possible over a retention interval during which the screen remained blank. At 1300 ms after the memory array onset, a single colored square (probe) was presented at one of the previously occupied locations; participants used a button press to indicate whether the probe was or was not the same color as the original square presented at that location. One-half of the trials were "same" trials, and the remaining half were "different" trials. The sequence of the trials was pseudo-randomly determined, and participants completed 80 trials for each set size. To estimate individuals' VWM capacity, a standard formula defined by Cowan (2001; p. 166) was used. More precisely, VWM capacity (K) was calculated for each set size by K = set size × (hit rate − false alarm rate). To obtain a single metric of VWM capacity for each individual, K estimates for supracapacity set sizes (i.e., set size 4 and above) was averaged (Kcd).

EEG recording. The EEG was recorded during the experiment using our standard recording and analysis procedures (McCollough et al., 2007), including the rejection of trials contaminated by blinks or large (>1°) eye movements. We recorded from 20 standard electrode sites spanning the scalp, including International 10/20 sites F3, F4, Fz C3, C4, Cz P3, P4, Pz, O1, O_2, PO3, PO4, POz, T5, and T6, as well as from nonstandard sites OL and OR (midway between O1/2 and T5/6). Our channels of interest were parieto-occipital channels (P3/4, O1/2, PO3/4, OL/R, T5/6, and POz) based on previous findings (Vogel and

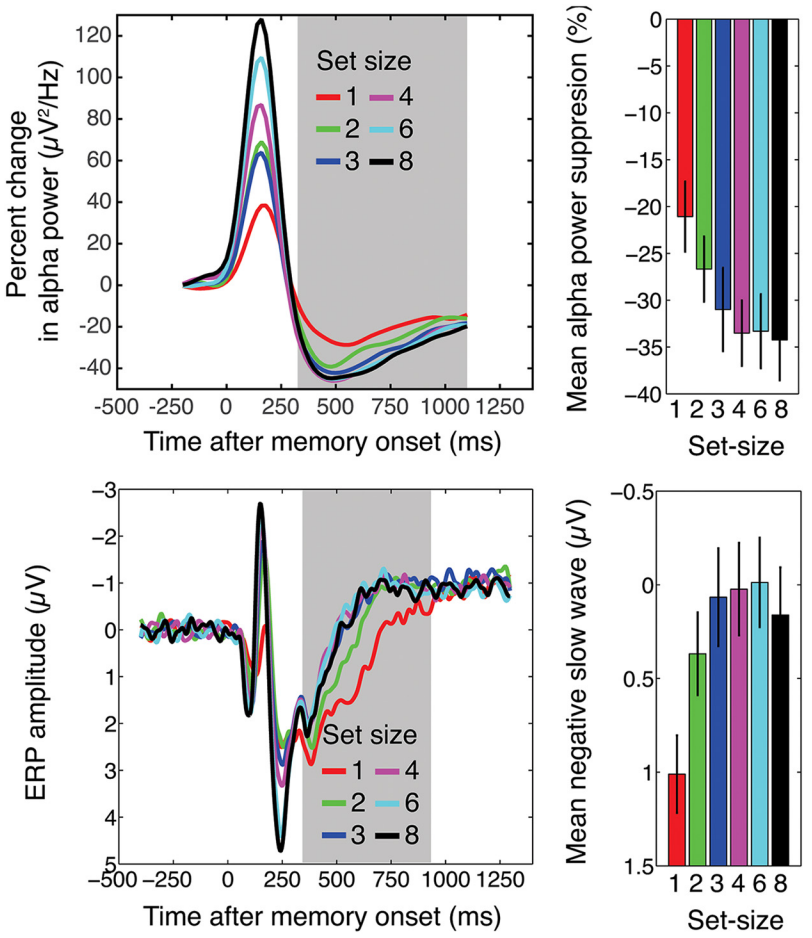

Figure 3. The α power suppression and the negative slow wave. Top, Averaged α power suppression observed at the parieto-occipital channels (P3/4, PO3/4, O1/2, OL/R, T5/6, and POz) after the onset of the memory array. Right, Mean α power suppression during the retention interval indicated by the gray box. Bottom, Averaged negative slow wave observed at the same posterior channels after the onset of the memory array. Right, Mean amplitude during the retention interval indicated by the gray box.

Machizawa, 2004; Vogel et al., 2005; Mazaheri and Jensen, 2008; van Dijk et al., 2010). Each trial was segmented into 400 ms pretrial and 1300 ms postmemory array onset epochs. Trials containing ocular artifacts, movement artifacts, or amplifier saturation were excluded from the analyses. Then, the data for each artifact-free trial were transformed into time-frequency domain by using sliding-window SFFT (spectrogram.m) with a fixed window size of 400 ms that was slid by 20 ms. As a result, each trial was converted to a series of 400-ms-wide spectrograms whose center ranged from −200 to 1100 ms. The resultant power spectrograms were averaged for each set size and baselined in the following manner: (1) the spectrogram observed during the baseline period [−400 to 0 ms time window (centered approximately −200 ms) relative to the onset of a memory array] was subtracted from all of the spectrograms; and (2) the difference spectrogram was then divided by the baseline spectrogram to calculate the relative change in the power.

ERP preprocessing. For ERP preprocessing, we used the same artifact-free trials as defined in EEG preprocessing (i.e., 400 ms pretrial and 1300 postmemory onset). Importantly, ERP data were not segmented into sliding time windows. The mean baseline (−400 to 0 ms before stimulus onset) amplitude was subtracted from EEG amplitude at each time point in the trial. The baselined trials were then averaged for each set size to create the ERP response for each condition.

Searching for an oscillatory correlate of VWM capacity. To find such an oscillatory correlate of VWM capacity limit, a class of bilinear functions with varying inflection points was fitted to every time-frequency data point to explain the set-size-dependent power modulation in the grand average spectrogram. The inflection point was allowed to vary from 2 to 8 (i.e., power value changes monotonically up to set size 8). The goal of this analysis was to find a power frequency band that showed a great fit ($r > 0.9$) with the bilinear function with the inflection point ~3 throughout the retention interval because it indicates that the power modulation at the frequency band shows the characteristic set-size function of VWM capacity.

Estimating α-phase-specific modulation during retention. We estimated the amplitude modulation specific to α phases in the following manner. First, we bandpass filtered the EEG data for each trial with 7–9 Hz and to estimate the instantaneous phase of the α activity by hilbert transform (hilbert.m). Then, we calculated the mean raw amplitudes during the retention interval (300–1300 ms after the onset of the stimulus) and during the baseline period (−400 to 0 ms before the onset of the stimulus) for 12 30°-wide, equi-width phase bins based on the estimated instantaneous phase. Those bins were −15 to 15°, 15–45°, 45–75°, 75–105° (containing α peak), 105–135°, 135–165°, 165–180 and −180 to −165°, −165 to −135°, −135 to −105°, −105 to −75° (containing α trough), −75 to −45°, and −45 to −15°. Then, the baseline mean amplitude for each phase bin was subtracted from the corresponding retention interval amplitude to calculate the phase-specific amplitude modulation.

Evaluating contribution of the sustained negativity and the α power suppression in explaining individual differences in VWM capacity. To test whether the sustained negativity and the α power suppression explains the shared or unique portion of variance in individual differences in VWM capacity, we did the following. First, we examined the adjusted R^2 values for two single-predictor models (i.e., the sustained negativity only and the α power suppression only as a predictor) and the double-predictor model (i.e., both the sustained negativity and the α power suppression as predictors) as well as the partial correlation coefficient for each predictor. Also, we tested the double-predictor model in a hierarchical manner to calculate the change in F statistics attributable to the addition of the secondary predictor in the model. We repeated this twice to test the effect of adding the sustained negativity and the α power suppression as the secondary predictor.

Experiment 2

Behavioral procedure. Experiment 2 was identical to Experiment 1 except for the following modifications. The memory array consisted of either one or three colored squares to remember. The retention interval lasted 1000 ms after the stimulus onset for one-half of the trials (short conditions) and 4000 ms after the stimulus onset for the other half of the trials (long conditions).

EEG recording and ERP preprocessing. The same recording parameters and preprocessing as Experiment 1 were applied except for the duration of trials. For short conditions, each trial was defined as −400 to 1000 ms after the stimulus onset, and for long conditions, it was defined as −400 to 4000 ms after the stimulus onset.

Results

Experiment 1

Behavioral results

Behavioral performance for each set size was first transformed using Cowan's K formula (Cowan, 2001). A repeated-measures ANOVA revealed that there was an expected set-size effect such that VWM capacity estimate monotonically increased up to set

size 4 (mean K = 0.95, 1.83, 2.49, 2.65, 2.64, and 2.49 for set sizes 1, 2, 3, 4, 6, and 8, respectively), reaching a plateau for higher set sizes (linear effect: $F_{(1,32)}$ = 68.6, $p < 0.001$; quadratic effect: $F_{(1,32)}$ = 114.1, $p < 0.001$). To compute individuals' VWM capacity estimate (Kcd), the K estimates for set size 4 and above were averaged together (mean Kcd = 2.59; SE, 0.12).

EEG results

When a class of bilinear function with freely varying inflection points was fit to the spectrogram across set sizes, we found that the power modulation of 7–9 Hz activity over the parieto-occipital channels (P3, P4, O1, O_2, OL, OR, PO3, PO4, T5, T6, and POz) was well characterized by bilinear functions with an inflection point of ~3–4 (Fig. 2). This robust fit was observed from 300 ms after the onset of memory array until the end of the retention interval. To evaluate the direction of the power modulation, we calculated the proportional change in power (microvolt squared per hertz) compared with the baseline period of the average power of 7–9 Hz activity across the parieto-occipital channels. This revealed that 300 ms after the memory array onset, parieto-occipital α power monotonically decreased as a function of a set size up to set size 3, plateauing at higher set sizes (Fig. 3). This event-related proportional decrease in power is defined as event-related desynchronization (ERD). A repeated-measures ANOVA for the mean parieto-occipital α power over a 300–1300 ms time window statistically confirmed this observation (linear effect: $F_{(1,32)}$ = 20.8, $p < 0.001$; quadratic effect: $F_{(1,32)}$ = 12.5, $p < 0.001$; Fig. 3).

Next, we tested whether the sustained α power suppression (ERD) was correlated with individual differences in VWM capacity estimates (Kcd). Figure 4 shows the correlations between Kcd and α power measures. Although there was no statistically significant correlation between Kcd and the α power measure at any single set size, when we quantified α power set-size effect as the difference between mean α power ERD for subcapacity set sizes (i.e., set sizes 1 and 2) and mean α power ERD for supracapacity set sizes (i.e., set sizes 4, 6, and 8), we found that the α power set-size effect was correlated with individual VWM capacity (R^2 = 0.22, $p < 0.01$; Fig. 4). More precisely, high-capacity individuals showed further suppression of α power in supracapacity set sizes than in subcapacity set sizes, whereas low-capacity individuals did not. Together, this suggests that the power of posterior α activity (i.e., 7–9 Hz) serves as a neural correlate of VWM capacity.

ERP results

As Figure 3 shows, we found that the negative slow wave over parieto-occipital channels (P3, P4, O1, O_2, OL, OR, PO3, PO4, T5, T6, and POz) showed a characteristic set-size effect. The mean negativity 300–1000 ms across the parieto-occipital channels after the memory onset increased up to set size 3 and stopped increasing as a function of set size thereafter (linear effect: $F_{(1,32)}$ = 18.8, $p < 0.001$; quadratic effect: $F_{(1,32)}$ = 30.4, $p < 0.001$). To examine whether the negative slow wave is sensitive to individual differences in VWM capacity, we examined the correlations between the magnitude of the negative slow wave and VWM capacity estimate (Kcd). Although there was no statistically significant correlation between Kcd and the amplitude of negative slow wave at any single set size, when we quantified the ERP set-size effect in the same manner as the α power set-size effect (i.e., mean ERP amplitude for subcapacity set sizes − mean ERP amplitude for supracapacity set sizes), we found that the ERP set-size effect was correlated with individual VWM capacity (R^2 = 0.19, p = 0.01; Fig. 5), indicating that high-capacity individuals showed a larger increase in the negativity for larger set sizes than low-capacity individuals. Thus, similar to the CDA, the negative slow wave satisfies the criteria for a neural correlate of VWM capacity limit.

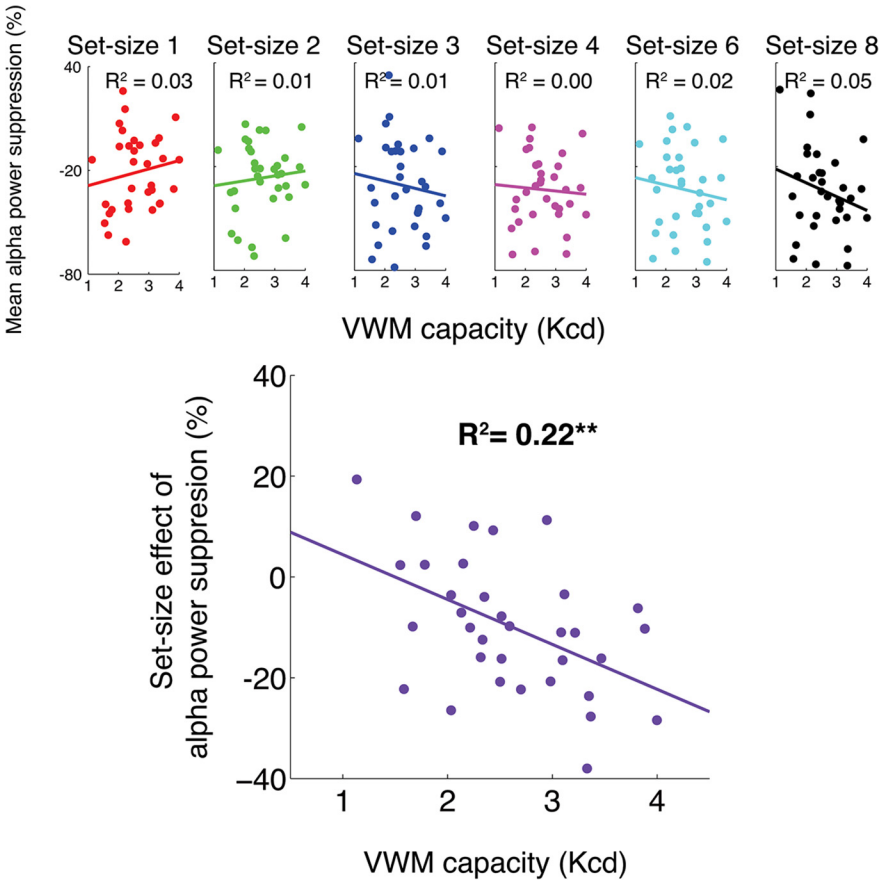

Figure 4. Correlations between the α power suppression and VWM capacity. Top Correlations between the α power suppression and VWM capacity (Kcd) across set sizes. Bottom, Correlation between VWM capacity and the set-size effect of the α power suppression. $^{**}p < 0.01$.

Examining phase-specific modulation of α activity

We then investigated whether the two neural correlates of VWM capacity are two manifestations of the same neural phenomenon. As noted previously, prior studies proposed that phase-specific modulation of α activity could provide a singular mechanistic explanation of both the negative slow wave and the sustained α power suppression. More precisely, both phenomena are expected when amplitudes at α peak are disproportionately suppressed while amplitudes at α trough are relatively unchanged (Mazaheri and Jensen, 2008; van Dijk et al., 2010). As Figure 6 shows, peak amplitudes of α oscillation

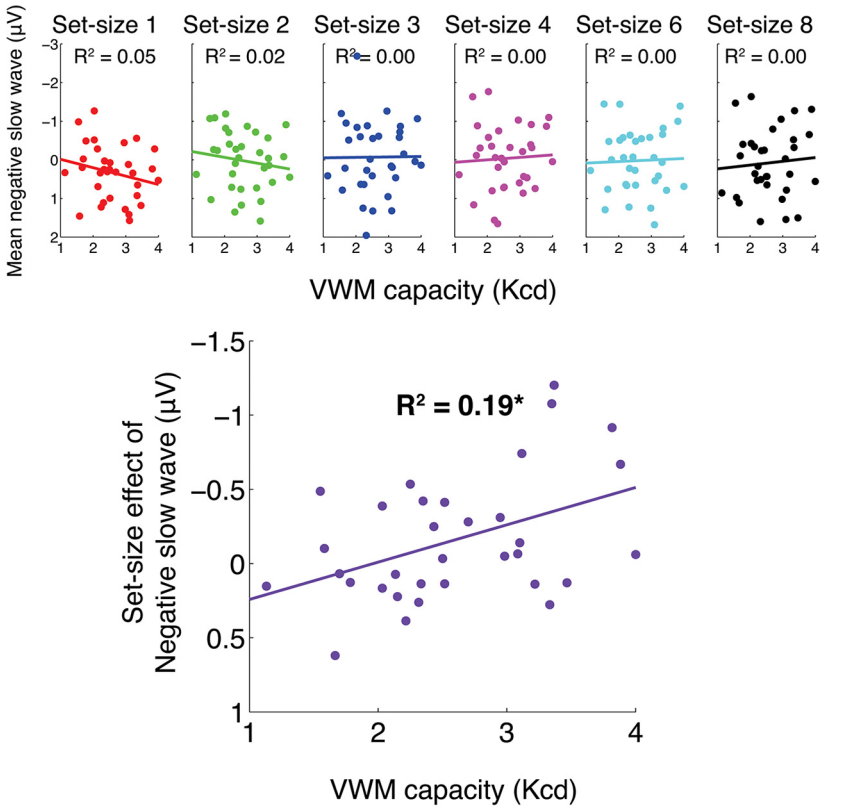

Figure 5. Correlations between the negative slow wave and VWM capacity. Top, Correlations between the negative slow wave and VWM capacity (Kcd) across set sizes. Bottom, Correlation between VWM capacity and the set-size effect of the negative slow wave. *$p < 0.05$.

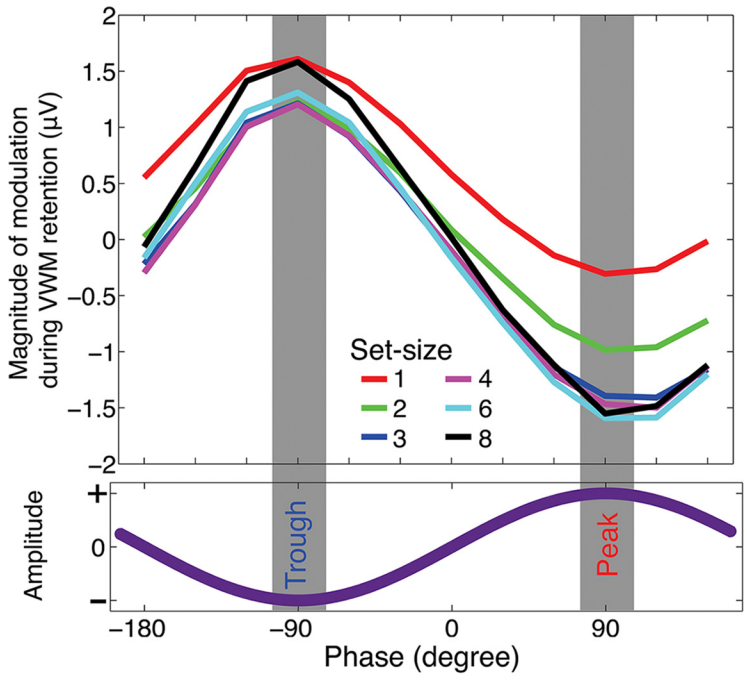

Figure 6. α-Phase-dependent modulation of EEG amplitudes during the VWM retention interval across set sizes.

were systematically suppressed to reveal the capacity-limited set-size effect (linear effect: $F_{(1,32)} = 32.9, p < 0.001$; quadratic effect: $F_{(1,32)} = 23.4, p < 0.001$). Interestingly, there was a large increase in trough amplitude, but its set-size effect was much smaller and did not conform to the capacity-limited set-size effect (linear effect: $F_{(1,32)} = 0.0$, n.s.; quadratic effect: $F_{(1,32)} = 10.1, p < 0.01$). Although this seems to be partially in line with the asymmetric modulation account, an alternative account assuming separate but co-occurring mechanisms for the negative slow wave and the sustained α power suppression could also explain this phenomenon. More precisely, the negative slow wave might be caused by a phase-unspecific (i.e., symmetric) negative DC shift that coincided with symmetric suppression of α activity (Fig. 7). To test apart these two hypotheses, we conducted Experiment 2.

Unique contributions of the negative slow wave and the sustained α power suppression to individual differences in VWM capacity

Next, we examined the functional relevance of the negative slow wave and the sustained α power suppression to VWM. If the two signals are merely two separate manifestations of a single neural mechanism (i.e., asymmetric α modulation), it is reasonable to expect that (1) they are correlated across all set sizes and (2) they explain the same variance in the individual differences in VWM capacity. On the other hand, if the two signals reflect separate VWM functions that contribute to individual differences in VWM, we would expect that (1) they are not correlated across set sizes and (2) they explain the unique portion of the variance. The results of correlational analyses supported the latter. First, we did not observe a significant relationship between the two signals constantly across set sizes except for set size 6 ($R^2 = 0.17, p < 0.05$; Fig. 8). More importantly, we observed no correlation between the set-size effects of the two signals ($R^2 = 0.00$, n.s.; Fig. 8), and each set-size effect uniquely contributed to explaining the variance in individual differences in VWM capacity (partial $r = -0.44$ and -0.48 for ERP and α power ERD set-size effect, respectively) Furthermore, using both signals as predictors significantly increased the amount of explained variance in individual differences in VWM capacity (adjusted $R^2 = 0.33$ compared with adjusted $R^2 = 0.20$ and 0.16 for ERD set-size effect and ERP set-size effect as a single predictor, respectively; $F\text{-change}_{(1,30)} = 7.3, p = 0.01$ when adding the ERP correlate as the secondary predictor, and $F\text{-change}_{(1,30)} = 8.9, p < 0.01$ when adding the α power correlate as the secondary predictor).

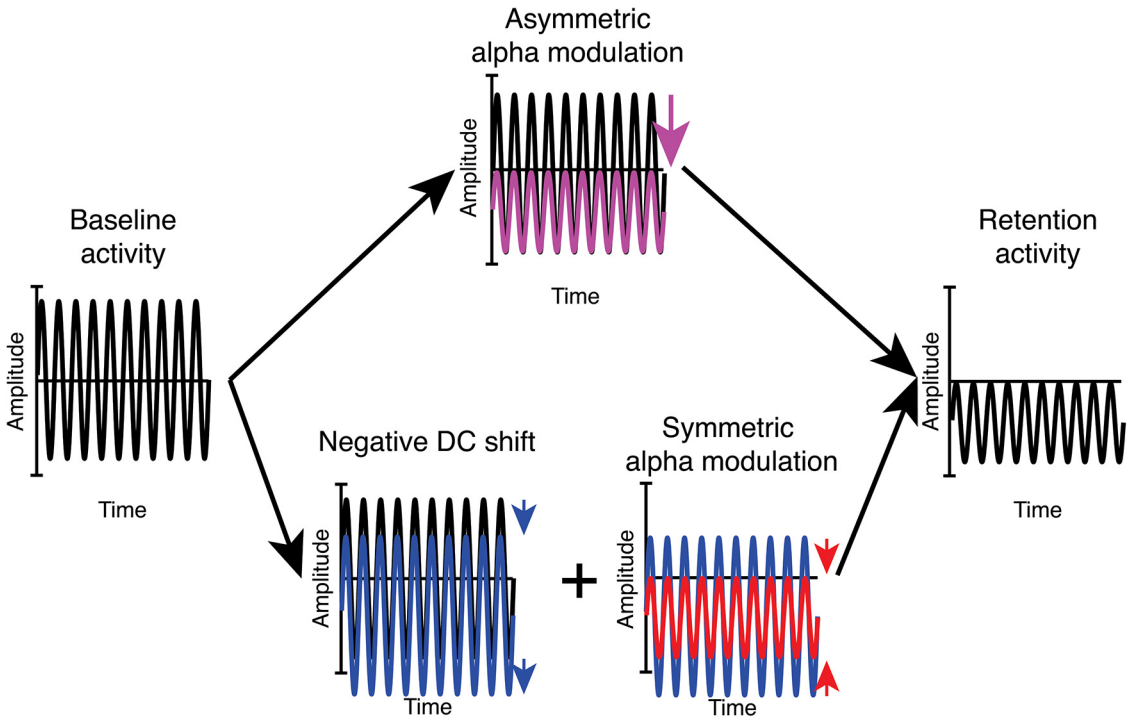

Figure 7. Asymmetric and symmetric α modulation of retention activity. Shown are two hypothetical mechanisms for the observed neural correlates of VWM capacity. The top flow depicts the asymmetric α modulation hypothesis, and the bottom flow depicts the DC plus symmetric α modulation hypothesis.

We found ERP and oscillatory correlates of VWM capacity, namely negative slow wave and sustained α power suppression, respectively. Previous studies suggested that these two signals might be two different manifestations of a singular neural phenomenon, namely asymmetric α modulations. Our correlational results showed that they are not correlated, and each neural measure uniquely contributed to explaining the individual differences in VWM. However, these correlational results are not sufficient to claim that these two measures are disociable because of the noisy nature of neural measurement. Thus, in Experiment 2, we attempted to obtain more direct evidence that the negative slow wave and the sustained α power suppression are differentially modulated. Here, we focused on the duration of each signal because we observed that the time window during which each signal was observable was noticeably different. In contrast to the negative slow wave whose set-size effect dissipated by 1000 ms after the memory array onset, the set-size effect for the sustained α power suppression lasted until the end of the retention interval. To examine this difference more thoroughly, we elongated the retention interval in Experiment 2. If the negative slow wave and the sustained α power suppression are two manifestations of asymmetric α modulation, then the two signals should show identical time courses. On the other hand, if they are two dissociable neural correlates of

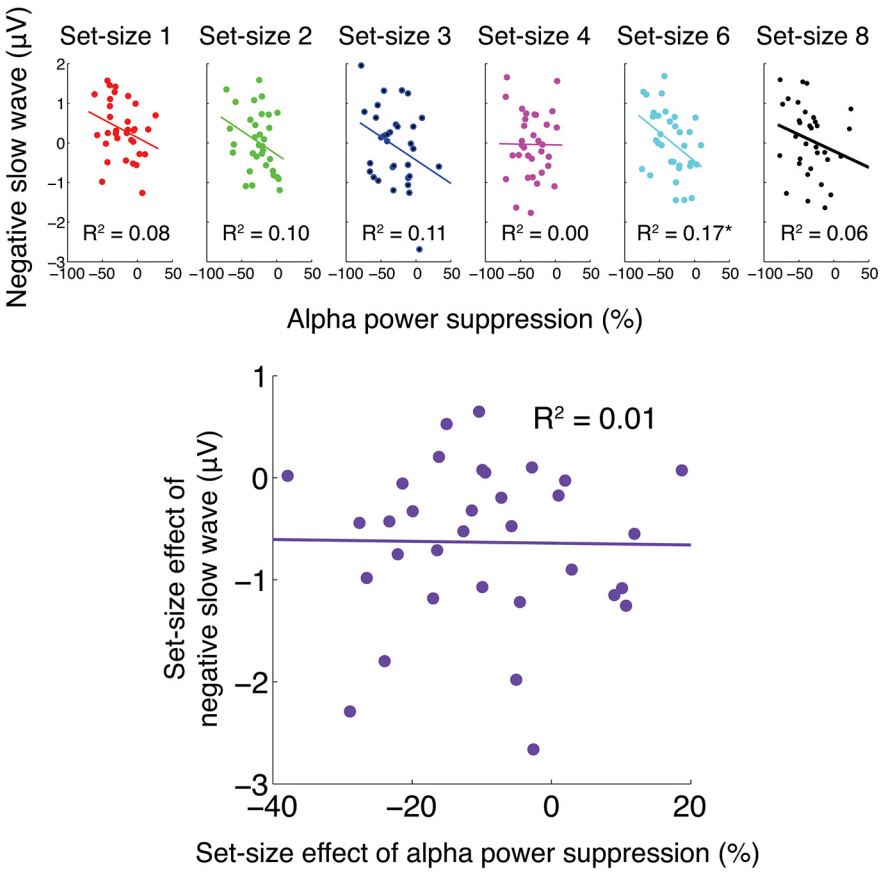

Figure 8. Correlations between ERP and α power correlates of VWM capacity. Top, Correlation between the negative slow wave and the α power suppression across set sizes. Bottom, Correlation between the set-size effects of the ERP and the α power correlates of VWM. *$p < 0.05$.

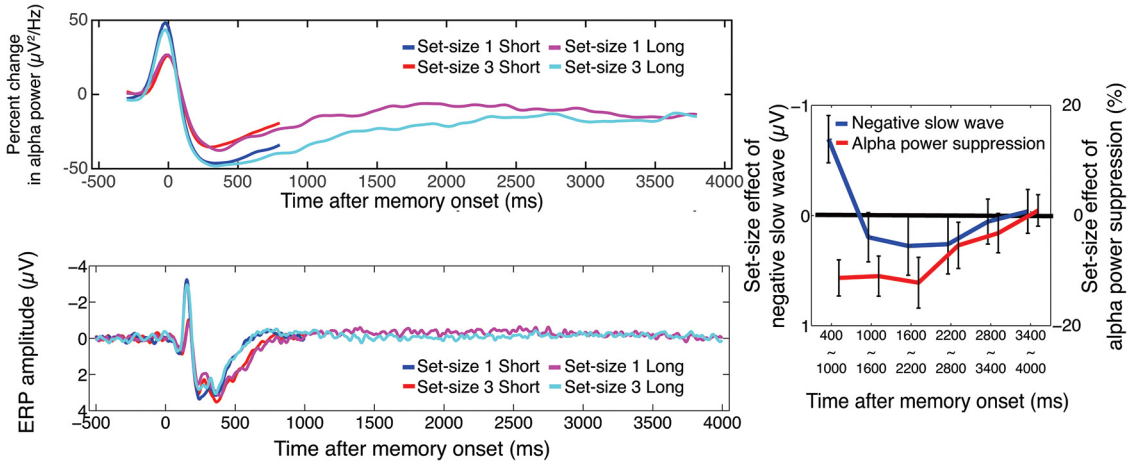

Figure 9. The results of Experiment 2. Left, The α power responses (top) and ERP responses (bottom) observed at the averaged parieto-occipital channels. Note that the *x*-axis for the α power plot indicates the center of the 400 ms time window. The right line graph shows the time course of the ERP and the α power set-size effect during the long retention interval.

VWM with close proximity in onset timings, then their durations might be different.

Experiment 2

Behavioral results

A repeated-measures ANOVA revealed a main effect of set size ($F_{(1,18)} = 363.2$, $p < 0.0001$) such that the *K* estimate was higher for set size 3 (mean $K1 = 0.96$ and 0.94 for short and long conditions, respectively, and mean $K3 = 2.47$ and 2.46 for short and long conditions, respectively); neither the main effect of retention duration nor the interaction were significant.

ERP results

As Figure 9 shows, we replicated the finding in Experiment 1. We observed that the negative slow wave observed at parieto-occipital channels (P3, P4, O1, O_2, OL, OR, PO3, PO4, T5, T6, and POz) was significantly larger for the set size 3 than for the set size 1 condition. To evaluate the time course of this effect, the retention interval in the long condition was partitioned to six bins (i.e., 400–1000, 1000–1600, 1600–2200, 2200–2800, 2800–3400, and 3400–4000 ms after the stimulus onset). The set-size effect was significant for both short ($t_{(18)} = 2.32$, $p = 0.03$) and long ($t_{(18)} = 3.21$, $p < 0.01$) conditions for the 400–1000 ms bin but was no longer significant thereafter.

EEG results

We focused our analysis on the power modulation of the α power (7–9 Hz) observed at parieto-occipital channels (P3, P4, O1, O_2, OL, OR, PO3, PO4, T5, T6, and POz). Figure 9 shows the time course of the α power modulation across conditions. First, we replicated the result from Experiment 1; the mean parieto-occipital α power during the short retention interval (400–1000 ms after the memory array onset) was lower for set size 3 than for set size 1 ($t_{(18)} = 3.29$, $p < 0.001$). More importantly, this set-size effect lasted much longer in the long retention condition. To statistically evaluate the duration of the set-size effect, we performed a series of paired *t* tests between the mean α powers for set sizes 1 and 3 for the prespecified bins and found that the contrast was statistically significant up to the 1600–2200 ms bin (*p* values <0.03). For the remainder of the retention intervals, although the set-size effect did not reach the statistical threshold, it showed a consistent trend. These results demonstrate that the set-size effect of the parieto-occipital α power suppression was much longer-lasting than the set-size effect of the negative slow wave.

Discussion

In this study, we simultaneously examined ERP and oscillatory correlates of VWM capacity to test whether the posterior negative slow wave and the sustained α power suppression show the capacity-defined set-size function in the absence of task-irrelevant distractors. In Experiment 1, we found that both the parieto-occipital negative slow wave and the sustained α power suppression showed that the capacity-defined set-size function and the magnitude of the set-size effects (i.e., supracapacity set sizes − subcapacity set sizes) were correlated with individual differences in VWM capacity. These findings are in line with the previous findings observed with lateralized VWM tasks and thus confirm that the two measures are truly reflecting the maintenance of VWM representations rather than filtering of task-irrelevant distractors.

Strikingly however, the two neural correlates showed qualitatively dissociable patterns. First, despite set-size effects of both measures correlating with behavioral performance, a regression analysis revealed that they do not correlate with each other and that they uniquely predict the separate sources of variance in the individual differences in VWM capacity. Since these correlational results by themselves are not sufficient to claim the dissociability of the two neural signals of VWM, we tested whether the negative slow wave and the sustained α power suppression are differentially modulated. Experiment 2 revealed that the α power suppression is much longer-lasting across the retention interval than the negative slow wave, thus providing converging evidence that the two signals are dissociable. Together, these findings are clearly inconsistent with the viewpoint that the negative slow wave and the sustained α power suppression are merely different manifestations of the same neural activity. Our results suggest that these two signals reflect dissociable neural processes, both of which uniquely contribute to determine an individual's behaviorally derived VWM capacity.

Two dissociable components in VWM capacity limit

What could the two neural signals reflect in determining individuals' VWM capacity? Recent studies using psychometric approaches have demonstrated that individual differences in VWM performance have primary contributions from two separable cognitive factors: attentional control and storage capacity (Unsworth et al., 2014). Even in a task without explicitly defined distractors, attentional control processes would be expected to be

critical for successful performance. These attentional control demands would likely increase as the number of items in the display exceeds the individual's capacity as a means to select a manageable subset of items for storage (Fukuda et al., 2015). Likewise, the ability to hold multiple individuated representations in an active state over the duration of the retention interval is also critical for successful performance. Whereas it is admittedly speculation at this point, the two neural measures reported have profiles that appear to map on to these two cognitive mechanisms contributing to capacity. For example, attentional control mechanisms would be expected to be most critical during the VWM encoding period, whereas storage capacity would be expected to play a critical role throughout the entire retention period. From this view, the shorter-lived negative slow wave during the encoding period and early retention period appears more in line with the expected timing of attentional control. In contrast, the α power suppression effect persisted mostly throughout the trial even for the long (3 s) retention interval and would thus be more consistent with mechanisms necessary for holding multiple items in an active state. One dominant account proposes that the α power suppression indicates the recruitment of a synchronized idle neuronal population. Indeed, the general pattern of the α power suppression that we have observed is consistent with this account. Recent studies provide a more specific prediction about the nature of the neuronal recruitment for representing multiple visual representations in mind. When holding multiple representations in VWM, it is critical to keep them "individuated" so that they won't contaminate one another. To do so, phase-coding models of VWM storage capacity proposes that each item is represented by synchronous activities in a low-frequency activity of participating neurons, and these synchronous activities coding each item are shifted in phase to avoid accidental synchronizations that could lead to confusion or misrepresentation of information (Raffone and Wolters, 2001; Siegel et al., 2009). As a result, the scalp EEG signal, which measures the sum of the phase-shifted signals, shows a set-size-dependent decrease in power up to the VWM capacity limit. Additional research, particularly measuring the activity of multiple object-coding neurons during VWM maintenance, would be necessary to directly test this hypothesis.

The contribution of other frequency band in VWM capacity limit

Other studies and theories have suggested the involvement of high-frequency signals (i.e., gamma frequency 30 Hz and above). Particularly, an influential model proposed by Lisman and Idiart (1995) proposed that mnemonic representations instantiated in the high-frequency activity are phase-locked to the low-frequency carrier wave. Although there are some EEG studies that showed partially consistent results with this proposal (Sauseng et al., 2009), no EEG study so far has provided a strong demonstration of the full model, possibly because of the technical disadvantage in acquiring high-frequency signals in scalp EEG signals (Yuval-Greenberg et al., 2008; Voytek et al., 2010). Considering these shortcomings, it is imperative that future studies obtain converging evidence from neural recording techniques that are sensitive to high-frequency neural activities (e.g., MEG, electrocorticography).

References

Cowan N (2001) The magical number 4 in short-term memory: a reconsideration of mental storage capacity. Behav Brain Sci 24:87–114; discussion 114–185. Medline

Fukuda K, Vogel EK (2009) Human variation in overriding attentional capture. J Neurosci 29:8726–8733. CrossRef Medline

Fukuda K, Vogel EK (2011) Individual differences in recovery time from attentional capture. Psychol Sci 22:361–368. CrossRef Medline

Fukuda K, Woodman GF, Vogel EK (2015) Individual differences in visual working memory capacity: contributions of attentional control to storage. In: Mechanisms of sensory working memory: attention and performance XXV (Jolicouer P, et al., eds), pp 105–119. San Diego: Academic.

Lisman JE, Idiart MA (1995) Storage of 7 ± 2 short-term memories in oscillatory subcycles. Science 267:1512–1515. CrossRef Medline

Luck SJ, Vogel EK (1997) The capacity of visual working memory for features and conjunctions. Nature 390:279–281. CrossRef Medline

Mazaheri A, Jensen O (2008) Asymmetric amplitude modulations of brain oscillations generate slow evoked responses. J Neurosci 28:7781–7787. CrossRef Medline

McCollough AW, Machizawa MG, Vogel EK (2007) Electrophysiological measures of maintaining representations in visual working memory. Cortex 43:77–94. CrossRef Medline

McNab F, Klingberg T (2008) Prefrontal cortex and basal ganglia control access to working memory. Nat Neurosci 11:103–107. CrossRef Medline

Raffone A, Wolters G (2001) A cortical mechanism for binding in visual working memory. J Cogn Neurosci 13:766–785. CrossRef Medline

Rouder JN, Morey RD, Cowan N, Zwilling CE, Morey CC, Pratte MS (2008) An assessment of fixed-capacity models of visual working memory. Proc Natl Acad Sci U S A 105:5975–5979. CrossRef Medline

Sauseng P, Klimesch W, Heise KF, Gruber WR, Holz E, Karim AA, Glennon M, Gerloff C, Birbaumer N, Hummel FC (2009) Brain oscillatory substrates of visual short-term memory capacity. Curr Biol 19:1846–1852. CrossRef Medline

Siegel M, Warden MR, Miller EK (2009) Phase-dependent neuronal coding of objects in short-term memory. Proc Natl Acad Sci U S A 106:21341–21346. CrossRef Medline

Unsworth N, Fukuda K, Awh E, Vogel EK (2014) Working memory and fluid intelligence: capacity, attention control, and secondary memory retrieval. Cogn Psychol 71:1–26. CrossRef Medline

van Dijk H, van der Werf J, Mazaheri A, Medendorp WP, Jensen O (2010) Modulations in oscillatory activity with amplitude asymmetry can produce cognitively relevant event-related responses. Proc Natl Acad Sci U S A 107:900–905. CrossRef Medline

Vogel EK, Machizawa MG (2004) Neural activity predicts individual differences in visual working memory capacity. Nature 428:748–751. CrossRef Medline

Vogel EK, McCollough AW, Machizawa MG (2005) Neural measures reveal individual differences in controlling access to working memory. Nature 438:500–503. CrossRef Medline

Voytek B, Secundo L, Bidet-Caulet A, Scabini D, Stiver SI, Gean AD, Manley GT, Knight RT (2010) Hemicraniectomy: a new model for human electrophysiology with high spatio-temporal resolution. J Cogn Neurosci 22:2491–2502. CrossRef Medline

Yuval-Greenberg S, Tomer O, Keren AS, Nelken I, Deouell LY (2008) Transient induced gamma-band response in EEG as a manifestation of miniature saccades. Neuron 58:429–441. CrossRef Medline

Zhang W, Luck SJ (2008) Discrete fixed-resolution representations in visual working memory. Nature 453:233–235. CrossRef Medline